

University of Arkansas, Fayetteville

ScholarWorks@UARK

Biomedical Engineering Undergraduate Honors
Theses

Biomedical Engineering

5-2019

Investigation of Acute Radiation-Induced Changes in Oxygenation in a Murine Breast Tumor Model

Alaa Abdelgawad

Follow this and additional works at: <https://scholarworks.uark.edu/bmeguht>



Part of the [Bioimaging and Biomedical Optics Commons](#), and the [Service Learning Commons](#)

Citation

Abdelgawad, A. (2019). Investigation of Acute Radiation-Induced Changes in Oxygenation in a Murine Breast Tumor Model. *Biomedical Engineering Undergraduate Honors Theses* Retrieved from <https://scholarworks.uark.edu/bmeguht/75>

This Thesis is brought to you for free and open access by the Biomedical Engineering at ScholarWorks@UARK. It has been accepted for inclusion in Biomedical Engineering Undergraduate Honors Theses by an authorized administrator of ScholarWorks@UARK. For more information, please contact scholar@uark.edu.

Investigation of Acute Radiation-Induced Changes in
Oxygenation in a Murine Breast Tumor Model

An undergraduate honors thesis
submitted to
the Department of Biomedical Engineering
College of Engineering
University of Arkansas
Fayetteville, AR

May 2019

By

Alaa Abdelgawad

Table of Contents

Abstract	3
Introduction	4
Methods	7
Results & Discussion	11
Conclusion	14
Acknowledgments	15
References	15

Abstract

Around 50-60% of all cancer patients undergo radiation therapy. Although some patients show complete response with no recurrence, a significant proportion of the population still develop radiation resistance. It is important to identify tumor resistance at early stages of therapy in order to adjust treatment protocol and avoid extra exposure to radiation. Current methods to assess treatment response are only limited to anatomical measurements of tumor volume after therapy. Novel approaches that shed the light on any functional information during the course of radiotherapy could significantly improve our ability to identify patients who do not respond to radiation therapy. Diffuse reflectance spectroscopy (DRS) is an optical fiber-based technique that is capable of quantitative, nondestructive, and repeated measurements of tumor biology. Our aim was to determine the sensitivity of DRS to escalating doses of radiation. An additional goal was to determine DNA damage and changes in hypoxic fraction post-radiation, and to determine if these immunohistochemical assessments were concordant with changes in optical properties, such as tissue scattering, hemoglobin concentration, and vascular oxygenation. Lookup table (LUT)-based model was used to fit the acquired DRS spectra and extract wavelength-dependent absorption and scattering properties from tissue. Our results have shown that the measurements of tumor optical properties such as oxygen saturation and total hemoglobin can provide reliable estimates of the hypoxic state of tissue. Additionally, we present significant increase in hypoxic fraction between control and irradiated groups.

Introduction

According to the American Cancer Society, about 268,600 new cases of invasive breast cancer will be diagnosed in 2019. Radiation therapy is usually recommended after lumpectomy because it lowers the risk of breast cancer recurrence¹. Radiation therapy destroys cancerous cells by depositing high-energy rays of photons (X-rays and gamma) or particles such as protons, neutrons and alpha². Radiation is commonly delivered through two mechanisms: externally using an outside source such as cathode ray tubes, linear accelerator or cobalt machines (external beam radiation), or internally by radioactive source inside the body using catheters or seeds (brachytherapy)³.

The overall outcome of radiation therapy is to cause functional abnormalities within the cell through direct and indirect actions, which eventually kills tumor cells over weeks of treatment. Presence of oxygen within cancerous cells is important to damage DNA and other macromolecules which are essential for cell survival. Tumor cells have developed multiple strategies to resist radiation damage. For instance, Hypoxia ($pO_2 < 10$ mg/Hg) significantly affects the outcome of radiation treatment and is associated with poor survival rates in cancer patient. Therefore, tumor hypoxia has been studied as a potential marker of developing resistance to radiation therapy³.

At this moment, there is no accepted technique that would enable early detection of radiation resistant tumors. Currently, imaging method used for assessing response to therapy such as Positron Emission Tomography (PET) imaging of ¹⁸F-Fluorodeoxy glucose (FDG) uptake or MRI are expensive and does not allow repeated measurements⁴. Moreover, PET imaging can be used only 5 or 6 weeks after therapy due to the limitation of radiolabeled isotope. Therefore, there

is an urgent clinical need for a viable technique that identify patients having poor response to radiation therapy on the early stage of the treatment⁵.

Current methods for measuring oxygen level within tissue are oxygen pO_2 microelectrodes, blood oxygen level dependent (BOLD) Magnetic resonance imaging (MRI), dynamic contrast enhanced (DCE)-MRI, PET imaging [18F]-labeled fluoromisonidazole (FMISO). The limitations of these current techniques are invasiveness level, ability for frequent measurements, and indirect assessment of tissue oxygen status. pO_2 microelectrodes are invasive, not capable of repeated clinical measurements, and measures hypoxia over a limited area of the tissue. Both MRI techniques provide indirect assessment of tissue oxygen level. Due to accumulation of FMISO contrast agent in normal tissue, this technique cannot be repeated frequently⁶. In contrast, diffuse reflectance spectroscopy (DRS) is an optical fiber technique which provides quantitative, non-destructive, and repeated measurements of tissue vascular oxygenation based on hemoglobin absorption⁷.

In DRS, light is generated by a halogen lamp light source and sent to the tissue through optical fiber probe. Fiber probe send the light from the source to the tissue and collect the reflected light back from tissue. The separation between the source and detector optical fibers determine the sampling depth. From the reflected light, tissue optical properties such as scattering, and absorption can be measured. The main tissue components that contribute to absorption are melanin in epidermis and hemoglobin located in blood vessels in the dermis. There are two types of hemoglobin in blood: hemoglobin bound to oxygen (oxygenated HbO_2), and unbound hemoglobin (deoxygenated dHb). Based on Figure 1, oxygenated and deoxygenated hemoglobin have

distinguishable absorption spectra over a wavelength range of 500-600 nm. Oxygenated hemoglobin has double peaks at 542 and 577 nm, while deoxygenated hemoglobin has a single peak at 560 nm⁸.

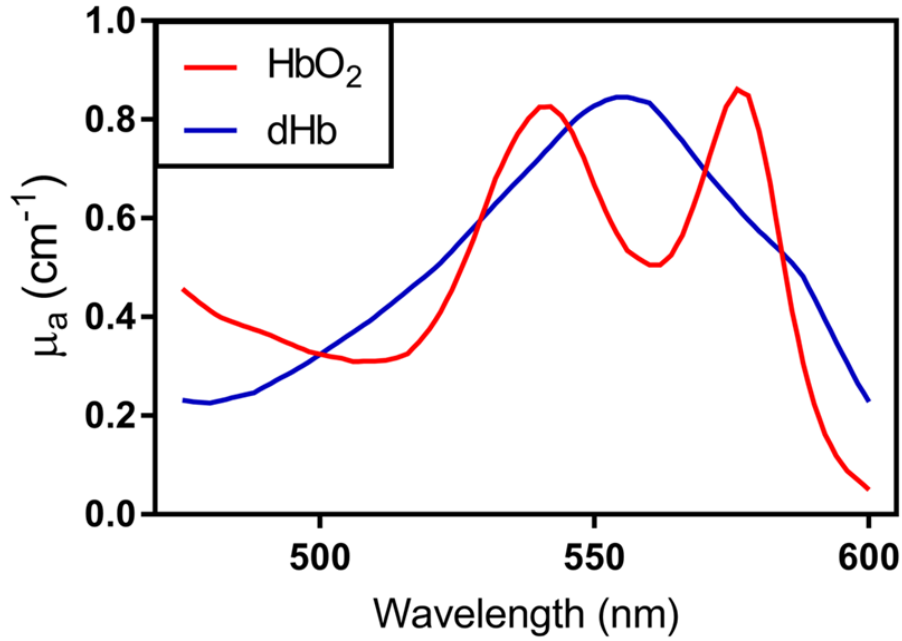


Figure 1: Absorption spectra of tissue components mainly contributing to the absorption of light in the range of 300-1000 nm: oxygenated hemoglobin(HbO_2), deoxygenated hemoglobin(dHb).

The vascular oxygenation (SO_2) can be quantified by calculating the ratio between oxygenated and total hemoglobin concentration as shown in equation 1:

$$SO_2 = \frac{HbO_2}{HbO_2+dHb} \times 100\% \quad \text{equ. (1)}$$

Absorption is described using an absorption coefficient $\mu_a(\lambda)$ as the following:

$$\mu_a(\lambda) = [cHb] [\alpha \varepsilon_{HbO_2}(\lambda) + (1 - \alpha)\varepsilon_{dHb}(\lambda)] + \varepsilon_{mel}(\lambda)c_{mel} \quad \text{equ. (2)}$$

Where cHb is total hemoglobin concentration, α is oxygen saturation, $\varepsilon_{HbO_2}(\lambda)$, $\varepsilon_{dHb}(\lambda)$, $\varepsilon_{mel}(\lambda)$ are the molar extinction coefficients of oxygenated hemoglobin,

deoxygenated hemoglobin and melanin, respectively. Similarly, scattering due to collagen, mitochondria, and nuclei can be described by scattering coefficient $\mu'_s(\lambda)$ as given in equation 3:

$$\mu'_s(\lambda) = \mu'_s(\lambda) + \left(\frac{\lambda}{\lambda_0}\right)^{-B} \quad \text{equ.(3)}$$

Where $\lambda_0 = 630 \text{ nm}$, and B is the scattering power related to scattering particle size. Consequently, reflectance is calculated as the ratio between the intensity of reflected light to that of the incident light⁹. DRS accuracy and sensitivity are mainly dependent on two factors: fiber optic probe source-detector separation, and lookup table LUT- based inverse model to extract optical parameters¹⁰.

The goal of this study is to determine the sensitivity of DRS to change in tumor oxygenation immediately after radiation. To achieve this goal, three aims were established:

1. Determine dose-dependent changes in tumor oxygenation using escalating doses of radiation (2Gy, 8Gy).
2. Determine depth-dependent radiation response using fiber optic probes with different source-detector separations.
3. Determine the correlation between immunohistochemical assessment of hypoxia and DRS optical properties after radiation.

Methods

Cell Culture and Tumor Xenograft

All studies and protocols were approved by the Institutional Animal Care & Use Committee (IACUC) of the University of Arkansas. Twenty-one balb/c mice were kept under standard 12 hours light and dark cycles at the Central Laboratory Animal Facility (CLAF). 4T1 murine mammary adenocarcinoma cells were injected into the mice (500,000 cells in 100 μ l) to grow subcutaneous tumor xenografts. When the tumor volume reached 200 mm^3 , DRS measurements were acquired on all mice. Tumors were excised from 5 mice in the control group. The other 16 mice were distributed into two groups to undergo radiation of 2 Gy (n = 10) and 8 Gy (n=6), respectively. Immediately after radiation, DRS spectra were recorded and mice were injected with pimonidazole, an established hypoxia marker (60 mg/kg, solution of 12 mg/ml). About 60 minutes post-injection, tumors were excised and snap-frozen in OCT compound.

Quantification of tissue optical properties

DRS consists of halogen lamp (HL-2000, Ocean Optics, Dunedin, Florida) as a light source, a USB spectrometer (Flame, Ocean Optics) for acquisition, and a fiber optic probe of source-detector separation of 1.5 mm and 2.25 mm as shown in figure 2. An established lookup table-based model (LUT) was used to quantify optical properties of tumor such as vascular oxygenation, hemoglobin concentration, and tissue scattering.

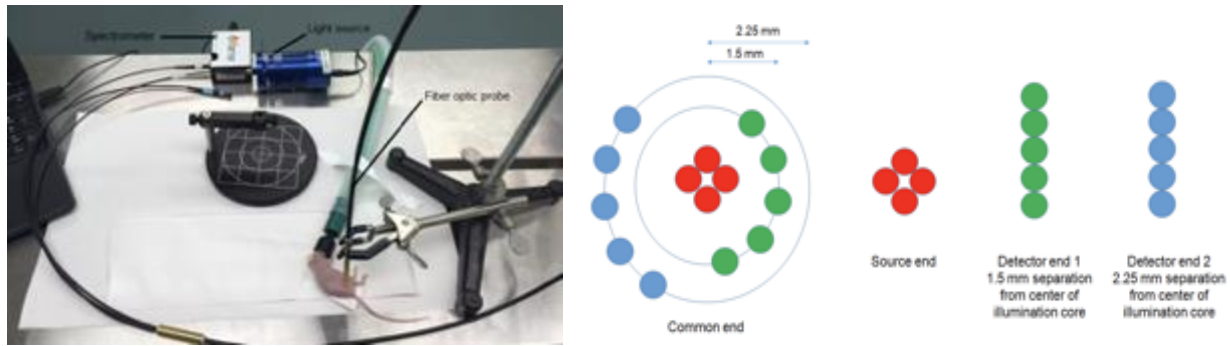


Figure 2: (A) Experimental setup of DRS and (B) bifurcated fiber optic probe illustrating the common tissue end, the source end that is connected to the light source, and the detector end that is connected to the USB spectrometer.

Immunohistochemical Assessment

Frozen tumors were stored -80 C and were sliced into sections of 10 μ m using a cryotome (CM 1850; leica, Inc., Nussloch, Germany). Based on the source-detector separation of 1.5 and 2.25 mm, tumor slices were obtained at depth ranges of (0.8-1.2 mm) and (1.4-1.8 mm), respectively. Direct labeling protocol was followed to stain with antibodies targeted to pimonidazole. First, slices were fixed with 4 % PFA, washed for three times with PBS (3 seconds each), and permeabilized with 0.1% Triton-X. Next, it was washed and incubated with blocking solution (95% PBS, 4% goat serum, and 1% sodium azide) for an hour in room temperature. Then, it was stained with primary antibody (Hypoxyprobe Red549 kit; HPI, Inc., Burlington, Massachusetts) for an hour in a dark room. After rinsing with PBS, slides were covered with fluoromount and stored in room temperature overnight for imaging.

Image and statistical Analysis

MATLAB (Mathworks; Natick, Massachusetts) was used to analyze immunofluorescence images at the specified depth ranges. First, each single image was converted into a grayscale image to find the local threshold using Otsu's method¹¹. Then, global threshold was calculated. Hypoxic fraction was computed by finding the ratio of segmented pixels (hypoxic) to the total pixels in tissue. All statistical analysis was performed using JMP (SAS, Cary, NC). Two-way ANOVA test was utilized to determine changes in hypoxic fraction of the three groups of interest at different depths. Linear correlation test was conducted to determine the relation between the optical properties and the immunohistochemical outcomes.

Results & Discussion

Figure 3a presents DRS spectra from control, 2 Gy, and 8 Gy groups which were collected when tumor volume reached 200 mm^3 . Similarly, Figure 3b presents wavelength-dependent absorption coefficient extracted from LUT model fit to DRS spectra. Our findings show the double peaks of at 542 and 577 nm appear less prominent in irradiated groups of 2 Gy and 8 Gy, which indicates lower levels of vascular oxygenation.

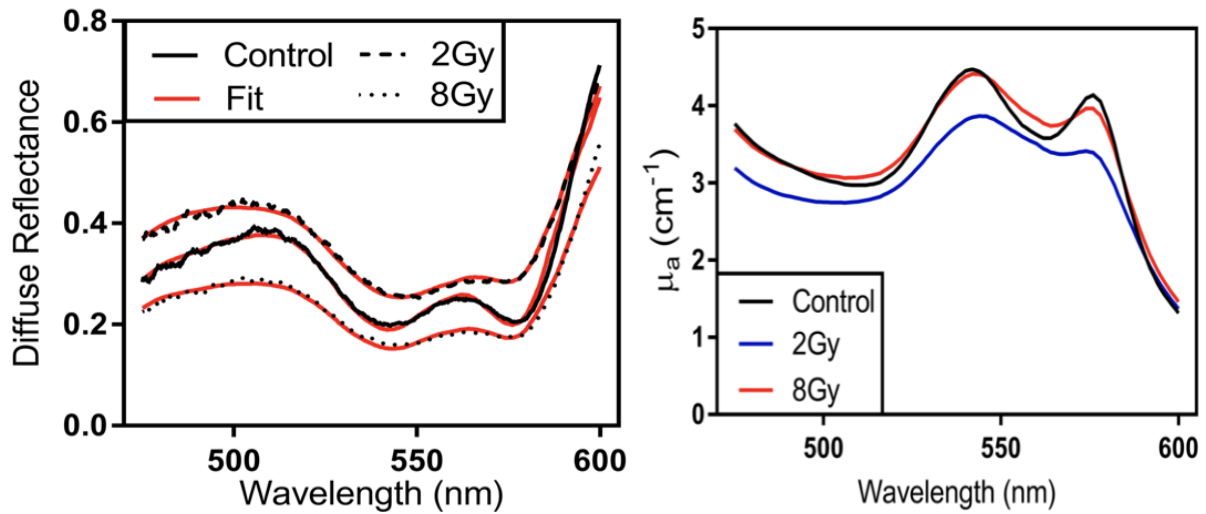


Figure 3: (A) Representation in vivo DRS spectra and their LUT fits from control, 2Gy, 8Gy groups at $V=200 \text{ mm}^3$. (B) Corresponding wavelength-dependent absorption coefficients determined from LUT fits to spectra.

Figure 4 represents the immunohistochemical images of hypoxic fraction in all of the three groups of interest at different depth ranges. Our results have shown an increasing trend in hypoxic fraction in response to radiation. We also investigated depth-dependent changes in hypoxia, but there was not a significant relation between HF and depth.

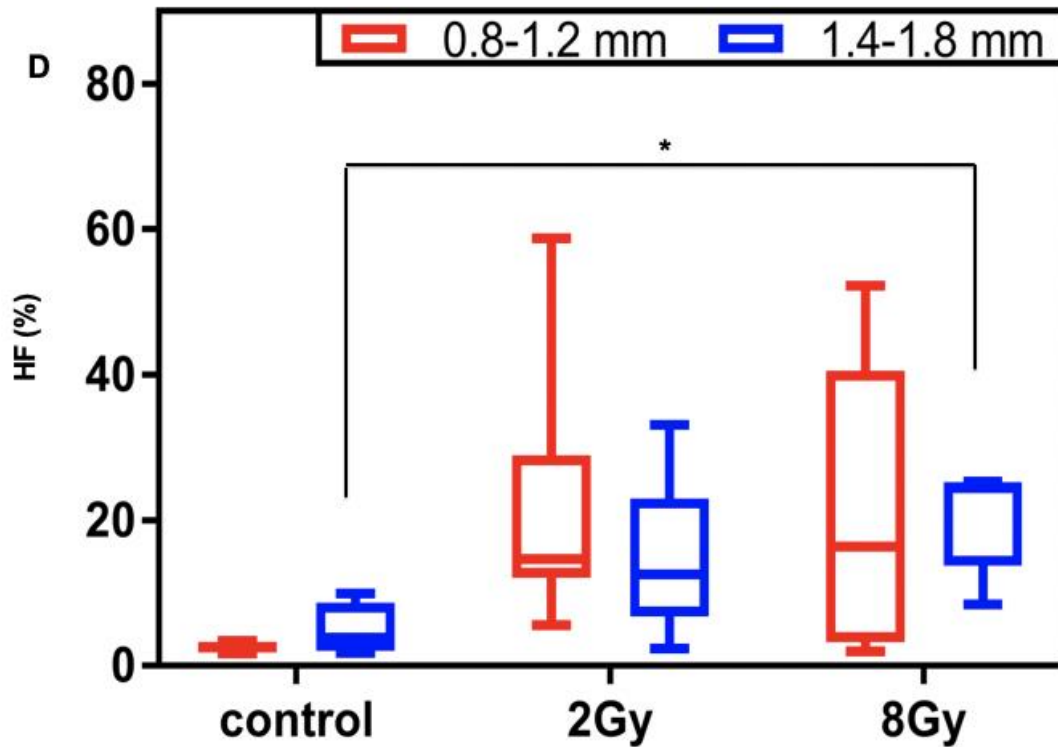
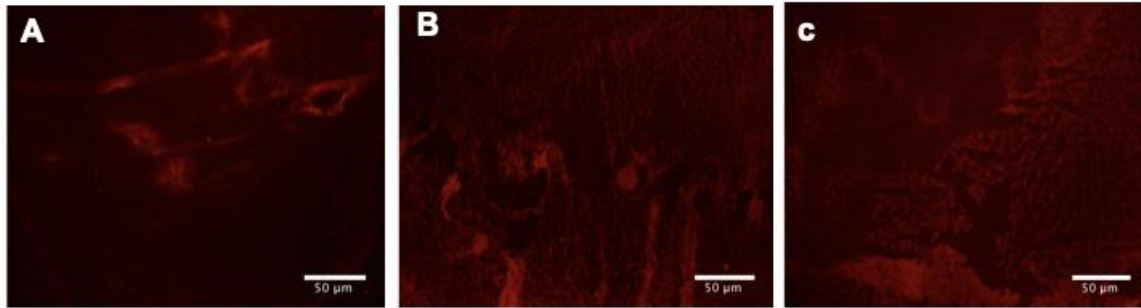


Figure 4: Pimonidazole immunofluorescence image of (A) control with HF= 4.66%, (B) 2Gy with HF= 14.67%, (C) 8Gy with HF= 21.95%. (D) Fold-change in hypoxia level of control, 2Gy, and 8Gy group with depth of (0.8-1.2 mm, and 1.4-1.8 mm). Error bars represent standard deviation. * represents p value ≤ 0.05

Figure 5 presents the changes of oxygen saturation among the three groups of interests at depth range of (0.8-1.2 mm) and (1.4-1.8 mm). Our findings show decreasing trend in oxygenation at the irradiated groups of 2 Gy and 8 Gy.

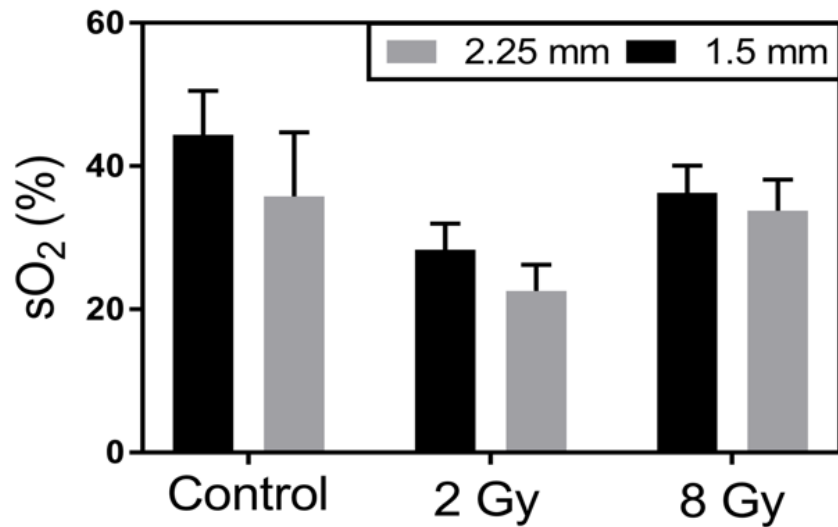


Figure 5: Shows mean values of oxygen saturation sO₂ (%) of control, 2Gy, 8Gy groups, collected at source-detector separation of 1.5 and 2.25 mm. Error bars represent SEM.

Based on pimonidazole bound areas in tissue and vascular oxygen saturation detected with quantitative optical Diffuse Reflectance Spectroscopy (DRS), a statistically significant negative correlation was found between hypoxic fraction and vascular oxygenation as shown in figure 6. Tumors with high oxygen saturation represents low hypoxic fraction and vice versa. These findings support that vascular oxygenation measured using DRS are concordant with hypoxic fraction and can be used as indirect indication of tumor oxygenation, which is consistent with previous findings in a similar xenograft model⁹.

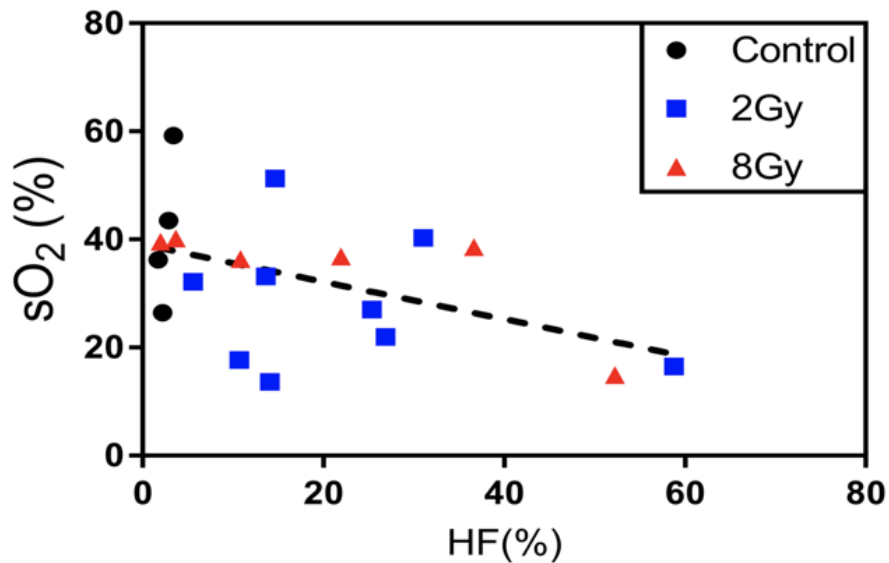


Figure 6: scatterplot representing the relationship between HF measure at depth of (0.8-1.2 mm) and DRS-based measures of sO₂ (%) collected at SD=1.5mm. Black solid line indicate regression line with $p=0.0395$, $R^2=0.226$.

Our future work includes plans to study time-dependent changes in tumor microenvironment in response to escalating doses of radiation. Hypoxic fraction increases after the exposure to radiation, we are currently investigating the mechanism behind this increase in hypoxia.

Conclusion

Radiation therapy has shown to be highly cost effective with a single modality treatment and accounts for about 5% of the total cost of cancer treatments. As a result, any improvement in radiation therapy efficiency will benefit a significant number of cancer patients. One of the main challenges in the modern oncology is tumor resistance against radiation treatment. DRS is a potential technique that may be used in assessing tumor response to radiation therapy at early stages of the treatment. In this study, we found that there were no significant depth-dependent changes in oxygen saturation or hypoxic fraction levels has been observed. However, there was

significant change in hypoxia in irritated groups of 2 Gy and 8 Gy. Monitoring vascular oxygenation can provide clinical assessment of tumor microenvironment during the course of the treatment.

Acknowledgments

We would like to acknowledge funding from the Honors College, the Jean Ostermeier Memorial Cancer Research Award, BMES travel award, and the Arkansas Biosciences Initiative.

References

1. Siegel, R. L., Miller, K. D., & Jemal, A. (2019). Cancer statistics, 2019. *CA: A Cancer Journal for Clinicians*, 69(1), 7-34. doi:10.3322/caac.21551
2. Read more about Breast Cancer Radiation Therapy at Susan G. Komen. (n.d.). Retrieved from <https://ww5.komen.org/BreastCancer/Radiation.html>
3. Baskar, R., Dai, J., Wenlong, N., Yeo, R., & Yeoh, K. (2014). Biological response of cancer cells to radiation treatment. *Frontiers in Molecular Biosciences*, 1. doi:10.3389/fmolb.2014.00024
4. Orth, Michael, et al. "Current Concepts in Clinical Radiation Oncology." *Radiation and Environmental Biophysics*. 2013;53(1):1-29.
5. Dietz A, Vanselow B, Rudat V, Conradt C, Weidauer H, Kallinowski F, et al. "Prognostic impact of reoxygenation in advanced cancer of the head and neck during the initial course of chemoradiation or radiotherapy alone." *Head & neck*. 2003;25(1):50-58.
6. Flood, A. B., Satinsky, V. A., & Swartz, H. M. (2016). Comparing the Effectiveness of Methods to Measure Oxygen in Tissues for Prognosis and Treatment of Cancer. *Advances*

in Experimental Medicine and Biology Oxygen Transport to Tissue XXXVIII, 113-120.
doi:10.1007/978-3-319-38810-6_15

7. K. Vishwanath et al., “Quantitative optical spectroscopy can identify long-term local tumor control in irradiated murine head and neck xenografts,” *J. Biomed. Opt.* 14(5), 054051-054051-4 (2009) [doi:10.1117/1.3251013]
8. T. Lister, P. A. Wright, and P. H. Chappell, “Optical properties of human skin,” *J. Biomed. Opt.* 17(9), [0909011–09090115 (2012) [doi:10.1117/1.JBO.17.9.090901].
9. Dadgar, S., Troncoso, J. R., & Rajaram, N. (2018). Optical spectroscopic sensing of tumor hypoxia. *Journal of Biomedical Optics*, 23(06), 1. doi:10.1117/1.jbo.23.6.067001
10. N. Rajaram, T. H. Nguyen and J. W. Tunnell, “Lookup table-based inverse model for determining optical properties of turbid media,” *J. Biomed. Opt.* 13, 050501 (2008).JBOPFO1083-3668 <https://doi.org/10.1117/1.2981797>
11. N. A. Otsu, “Threshold selection method from gray-level histograms,” *IEEE Trans. Syst. Man. Cybern.* 9, 62–66 (1979).ISYMAW0018-9472
<https://doi.org/10.1109/TSMC.1979.4310076>